Environmental Earth Sciences (2024) 83:337
https://doi.org/10.1007/s12665-024-11593-3

ORIGINAL ARTICLE

Relation between the soil erosion cover management factor and vegetation index in semi-arid basins

Mohamed Mahgoub[1] · **Ezzat Elalfy**[2] · **Hoda Soussa**[2] · **Yehia Abdelmonem**[2]

Received: 11 December 2023 / Accepted: 7 April 2024 / Published online: 15 May 2024

Abstract

The cover management factor is one of the main five factors that is used within the universal soil loss equation to reflect the effect of cropping and management practices on soil erosion rates. It is determined through tables and equations derived in tropical and European conditions, which are not suitable for semi-arid regions with different climate, topography, and soil characteristics. Therefore, this study considers al-Arish basin in Sinai Peninsula, Egypt as a semi-arid study area to generate a cover management factor's equation in terms of the Normalized Difference Vegetation Index using hydrological modeling and satellite images processing. To verify the proposed equation, it was applied to the Derna catchment in Libya and compared with European and tropical ones with respect to the hydrological outputs. Statistical analysis indicates that the proposed equation determines the cover management factor more accurately than those developed for tropical or European regions, as the correlation coefficient between the cover management factor and the hydrological results was 0.71, while it was about 0.20 for the European and tropical, equations, also the degree of agreement between the proposed equation's results and the hydrological simulation was 0.768 while it was 0.001 and 0.02 for the tropical and European equations respectively. By utilizing the newly developed equation, the soil erosion can be estimated more accurately for the semi-arid regions, and a better understanding of the relation between the vegetation cover and soil erosion can be drawn.

Keywords Cover management factor · NDVI · Remote sensing · Satellite images · Semi-arid regions · Soil erosion · Basin

Introduction

Soil erosion is one of the main natural environmental phenomena that leads to land degradation. It drifts the top layer of the earth and moves it from one place to another by the action of water and sometimes winds (Kumawat et al. 2021). It leads to the collapse of roads, artificial channels, and structures and even endangers human lives. In addition, it decreases the agriculture productivity, lessens the soil fertility, and reduces the levels of the basic plant nutrients needed for crops (Majoro et al. 2020). The Food and Agriculture Organization (FAO) indicated that the loss of soil productivity due to soil erosion affects up to 65 percent of the African agricultural lands (Centeri 2022). The amount of the soil eroded is usually calculated using the universal soil loss equation (USLE) and its revised model (RUSLE).

One of the most important factors in these equations is the Cover Management Factor (C-Factor), which indicates how land uses and management affect the runoff and soil erosion rates. It reflects the human activities via deforestation, urbanization, and agricultural practices that can

✉ Mohamed Mahgoub
mohamed_mahgoub@nwrc.gov.eg;
engmhmd.mahgoub@yahoo.com

Ezzat Elalfy
ezzatelalfy@gmail.com

Hoda Soussa
hoda_soussa@eng.asu.edu.eg

Yehia Abdelmonem
drhanirrdrain@eng.asu.edu.eg

[1] National Water Research Center NWRC, Water Resources Research Institute WRRI, Ministry of Water Resources and Irrigation MWRI, Ismailiya Canal, Shoubra El-Kheima, Qalyubia 13411, Egypt

[2] Irrigation and Hydraulics Department, Faculty of Engineering, Ain Shams University, Cairo, Egypt

accelerate the rate of soil erosion. The value of the C-Factor increases in the case of bare fallow areas, while it decreases in case of forests. The importance of the vegetation index is represented in dissipating the kinetic energy of the raindrops before impacting the soil surface, which reduces the amounts of surface runoff and decreases the soil loss rates. Thus, vegetation cover and cropping significantly influence the runoff and erosion rates. For instance, soil loss rates decrease exponentially as vegetation cover increases. Also, vegetation cover has a role in preserving soil characteristics, as it hinders the movement of water, contributes to protecting the soil against rainfall erosivity and surface sealing phenomena. Soil loss due to erosion poses a serious challenge to increasing agricultural productivity, as soil erosion leads to a decline in soil fertility at alarming rates. Increasing vegetation cover increases soil organic matter and stabilizes soil structure. It also protects the soil from direct exposure to sunlight and rain, which preserves the soil from dryness and erosion.

Many researchers have studied the effect of vegetative protection and cover management factor on soil erosion and soil organic carbon content. Imamoglu and Dengiz (2017) integrated the RUSLE with the geographic information system (GIS) to estimate the annual soil loss and to explain the effect of soil erosion on the soil organic carbon rates in the Alaca catchment in black sea region of Turkey. They investigated the effect of land use/cover, soil properities, and topographical features on soil erosion rates. They concluded that the distribution of soil erosion losses was directly correlated with the soil carbon losses, also they indicated that soil and topographical features affected the potential soil and the soil organic rates more than the type of land use/cover. Soil loss rates can be reduced by controlling the value of the C-Factor, as rainfall erosivity (R), soil erodibility (K), slope length (L), and steepness (S) depend on ground nature, while support practices (P) depends on contour farming and terracing which require considerable financial investment. Therefore, decision makers can use the C-Factor to identify areas that are most vulnerable to soil erosion, reduce soil loss rates, prevent the loss of nutrients, and to preserve soil organic carbon (Panagos et al. 2015).

Satellite images have recently been used to detect the changes of the vegetation cover, the Normalized Difference Vegetation Index (NDVI) is a measure to the amount of green vegetation using the spectral reflectance difference between Red and Near Infrared (NIR). Plant information is monitored using multispectral images with more rapid and accurate characteristics (Lee et al. 2021). Sun et al. (2018) applied the RUSLE model to investigate the soil loss rates on the Tibetan Plateau located in south west of China from 1984 to 2013 and reported that the soil erosion was very high. Ayalew et al. (2020) used the NDVI to determine the spatiotemporal variations of the C-Factor and detected the sensitivity of NDVI to various biophysical variables such as soil condition, topographic conditions, and crop growth stage. Balouei et al. (2021) detected the changes in land-use and land-cover in the Doiraj basin in Iran to estimate their impacts on soil erosion rates. They used meteorological data and remote sensing satellite images and found that the average rates of soil erosion in the years 1995, 2006 and 2015 in tons/hectare/year were 77.04, 91.51 and 108.94, respectively. Mu et al. (2022) demonstrated the soil erosion dynamics across the Grand Pearl River basin in southern China using continuous Landsat satellite image dataset over the past 30 years from 1990 to 2020 based on the RUSLE model, they estimated the C-Factor based on the NDVI. The results showed that the NDVI simulated the vegetation coverage well and displayed a decreasing trend of soil erosion over the past 30 years with an annual decreasing rate. Yu et al. (2023) investigated the tempo-spatial variabilities of vegetation coverage of the Kherlen River Basin in China. They applied the autoregressive moving average model and the breaks for additive season trend in the basin to analyze the temporal variations of NDVI from 2000 to 2020.

Most of the previous studies estimated the C-Factor using either guiding tables or equations derived in tropical, and European conditions, or imposed the values of the C-Factor for bare soil and forests. Karaburun (2010) investigated a relation between the C-Factor and NDVI derived from Landsat 5 in Buyukcekmece watershed in Istanbul. The C-Factor values for forest and bare soil were assumed to be 0 and 1, respectively, then a regression analysis was applied between the C-Factor and NDVI. The results showed the presence of large portions of areas with C-Factor values range between 0.2 and 0.4. Der Knijff et al. (2000) derived an equation to estimate the C-Factor for European climate conditions (C_{VK}), while, Colman et al. (2019) introduced equations for tropical climate conditions (C_{rA}). Almagro et al. (2019) compared results of the two C-Factor approaches of Der Knijff and Colman with the literature C-Factor values (C_{LIT}) of Guariroba basin, Brazil. Findings showed that the C_{rA} was capable to present similar values to C_{LIT} with percent bias of − 28%, while the C_{VK} was not performed well and showed a percent bias of 328%.

Arid and semi-arid areas cover approximately 40% of the land surface (Vasquez-Mendez et al. 2011), these regions suffer severe rainfall and soil erosion and deterioration of soil fertility due to the lack of the vegetative protection resulting from the climate variability and extreme occurrences such as floods and droughts. Tribak et al. (2009), Driss and Brahim (2018), and Zakariae and Abdellatif (2021) estimated the C-Factor and investigated the land cover changes at Wadi Tlata, Wadi Isly, and Wadi Lahdar in Morocco, respectively. They applied the USLE and used GIS and Remote sensing applications, and reported a significant decrease in cereal areas due to a considerable extension of

the eroded soil. Also, Okacha and Salhi (2023) proposed novel model to estimate the cover management factor across different climatic zones using the Five-Parameter Logistic (5PL) function. They compared their results with values of the literature-based C-Factor. The findings showed that the proposed models were in good agreement with literature C values.

Few studies have calculated the C-Factor within semi-arid regions, these studies relied on literature guiding tables or assumptions, and did not conduct innovative ways to obtain C-Factor values. Therefore, this study aims to calculate the C-Factor for semi-arid regions using new approach that combines hydrological analysis with remote sensing and GIS to get a relationship between the C-Factor and the NDVI for semi-arid basins. Wadi al-Arish in Sinai, Egypt, was considered as a case study representing the semi-arid catchments, as it contains all kinds of vegetation covers that may exist in the dry basins, such as trees, flooded vegetation, crops, built area, bare ground, and range lands, the hydrological outputs were used as a reference to compute the C-Factor due to the difficulty of obtaining field observations, which require hard cadastral surveying in addition to their existence in wide and remote areas. To ensure the validity of applying the proposed equation in semi-arid basins, it was applied to the Derna Valley in Libya. The results were compared with those of European and tropical conditions to obtain the most optimal equation representing the cover management factor for semi-arid basins. This relation will help in better understanding the effect of vegetation cover on the soil erosion.

The remainder of the paper is organized as follows: Materials and methods, Results and discussion, and finally Summary and conclusions.

Materials and methods

This study can be achieved by applying five stages; the first stage is collecting the hydrographic data and the hydrological records of Wadi al-Arish, Sinai Peninsula, Egypt. The second stage is to download the land cover to determine the NDVI values. The third stage is to apply the hydrological model to estimate the C-Factor values within the study area. The fourth stage is using the ARC-GIS-10.8.2 to generate a regression equation between the C-Factor and the NDVI. The fifth step is to verify the accuracy of applying the proposed equation in one of the semi-arid basins, which is Derna Valley in Libya, and to compare its outputs with the results of the C-Factor's equations used in European and tropical conditions, see Fig. 1.

Study area

Wadi al-Arish

Description of Wadi al-Arish Wadi al-Arish is the longest valley in Sinai Peninsula in Egypt, it occupies about one third of its area and extends for 250 km from the middle of Sinai to the Mediterranean Sea, covering an area of 23,300 km^2 between 29° 00′ N and 31° 00′ N, and 33° 05′ E and 34° 45′ E. It is an arid to semi-arid region which is characterized by hot weather of mean annual temperature of 22 °C. It is the highest in August at 29 °C and lowest in January at 13 °C, except for the coastal zone of a moderate climate similar to other regions in the eastern Mediterranean. Precipitation values decreases from the northeast towards the southwest, the greatest amount of

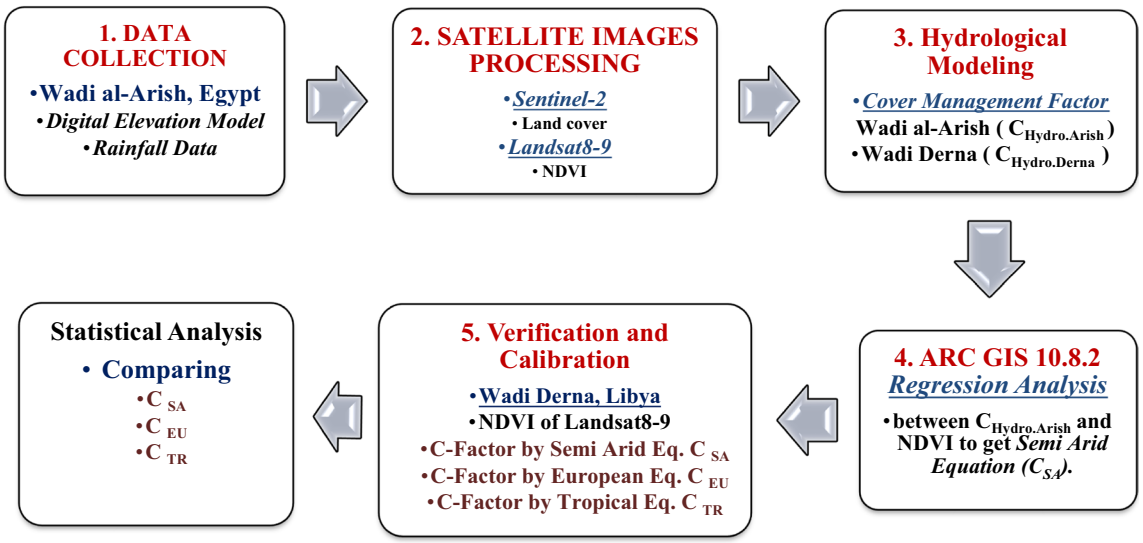

Fig. 1 Schematic diagram for the study procedures

the annual rainfall was found at Rafah station (304 mm) in the northeast and the annual rainfall average is about 120 mm along the Mediterranean coast. In the southern region, the annual rainfall reaches 20 mm in the coastal areas over the Gulfs of Aqaba and Suez and increases to 70 mm over the mountainous regions. it originates from the heights of the Al-Agma mountains and runs in the middle of the land of the labyrinth, penetrating its mountains, then the land of North Sinai, which takes the northeastern direction, following the general slope of the earth's surface until it reaches the shore of the Mediterranean Sea in the coastal city of al-Arish as shown in Fig. 2a. It is exposed to flashflood waters continuously, the most intense was in 2010.

Topography and Geology of Wadi al-Arish Limestone sedimentary rocks cover the entire drainage basin of Wadi al-Arish. The existence of cracks and joints increases the rate of water loss from surface runoff. Its southern topography is a tough terrain with rugged, sharp, and high-rise granite mountains with high elevations reaching more than 1600 m above sea level as shown in Fig. 2b. The central part contains al-Tih and al-Ajmah plateaus, both deeply indented and dipping towards the north as a wedge-shaped block section with its base along the Mediterranean Sea coast to the north and its tip surrounded by the Gulfs of Aqaba at the east and of Suez at the west (El Afandi et al. 2013).

Wadi Derna

Description of Wadi Derna Derna Valley in Libya was chosen as one of the semi-arid valleys, it is characterized by the topographic features and climatic conditions that distinguishes semi-arid basins, and contains various categories of land covers such as trees, cultivated crops, bare soils, range lands, and built areas. It leads down from the Jebel Akhdar mountains to the port city of Derna. It is located between two circles of 32° 34′ N and 32° 48′ N, and 21° 59′ E and 22° 38′ E as shown in Fig. 3a. It is 75 km long and drains a drainage basin of 575 km^2. In September 2023, the rainfall from the Storm Daniel led to the collapse of two dams across the river, causing catastrophic flooding in the city of Derna, which killed about 4000 people. It was one of the deadliest dam failures in history.

Derna has a hot, semi-arid climate with strong Mediterranean influences where all modest annual rainfall falls mainly between October and March, the average annual

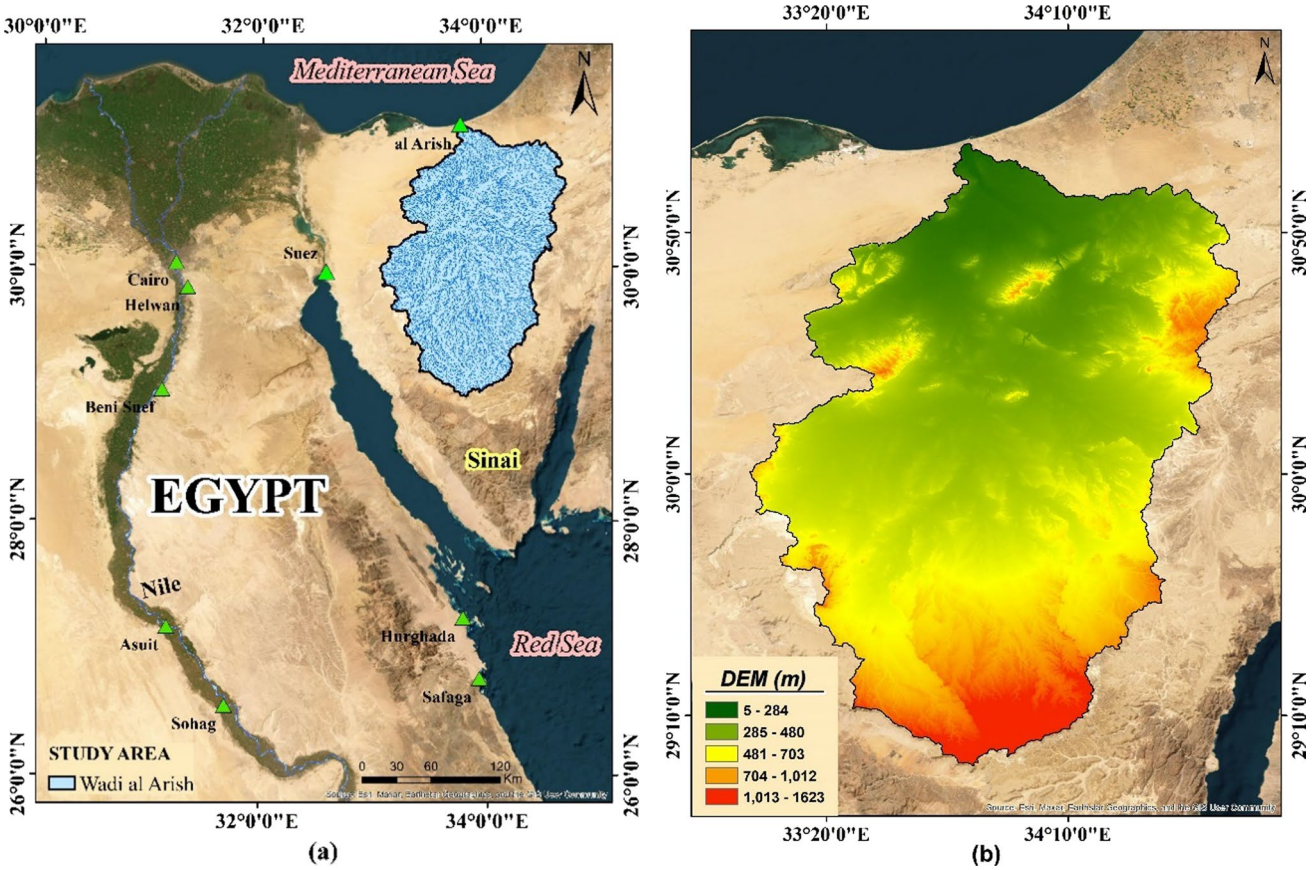

Fig. 2 Description of Wadi al-Arish, Sinai Peninsula, Egypt. **a** The location, **b** the DEM

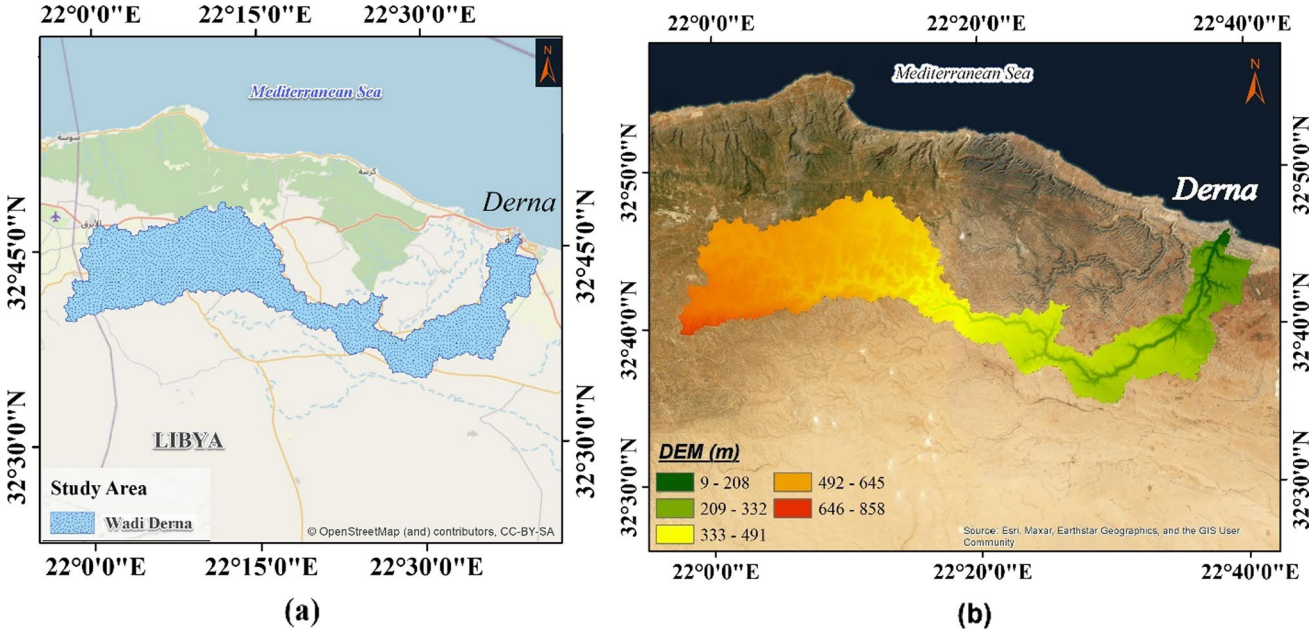

Fig. 3 Description of Wadi Derna, Libya. **a** The location of the watershed, **b** the DEM

rainfall is about 275 mm. In winter, the average temperature in the city ranges between 9 and 20 °C. Summer season is hot and effectively rainless, with the average temperature hovering well above 27 °C between June and October. The Akhdar Mountains stretch along the coast between Al-Marj and Derna. These limestone mountains rise steeply from the coast to about 600 m and then stretch about 30 km inland, reaching nearly 900 m at their highest points (Ashoor 2022), see Fig. 3b.

Data collection of Wadi al-Arish

Data with different types and different sources was collected. Details about data collection are shown in this section:

Digital Elevation Model (DEM): was downloaded with spatial resolution of 30 m using satellite images processing techniques from website https://earthexplorer.usgs.gov/ as shown in Fig. 2b.

Rain Gauge Data: was collected from the Egyptian Meteorological Authority (EMA). Figure 4a shows the available Meteorological stations located in Sinai, the average rainfall depth was estimated using the Thiessen polygon method of al-Arish, Nakhel and Al-Hasana rainfall stations.

Land Cover: Sentinel-2 images were used to generate different classifications of land-cover such as water, trees, flooded vegetation, crops, built area, bare ground, and range land (see land-use/land-cover, LULC, in Fig. 4b for Sentinel-2). Sentinel-2 provides free imagery with spatial resolution of 10 m available for the globe through Copernicus Open Access Hub site, https://scihub.copernicus.eu/dhus/#/home.

Methodology

Hydrological study supported by multiple software packages were applied as follows:

- The Watershed Modeling System (WMS) used morphological and metrological data to define basin's characteristics of Wadi al-Arish.
- $C_{\text{Hydro.Arish}}$; represents the cover management factor calculated by the hydrological model within the study area of Wadi al-Arish, Sinai, Egypt.
- HEC-HMS estimated the $C_{\text{Hydro.Arish}}$ for each type of land-cover (Fig. 5a) depending on the Curve Number (CN) derived from the soil conservation method.
- Arc-GIS is used for post-processing. It presents the coverage data over maps of the basin area based on Inverse Distance Weighting (IDW) interpolation method.
- Following Jiang et al. (2006), NDVI of Landsat 8–9 with 30 m spatial resolution, spanning the period of January 2023 (Fig. 5b) was calculated by computing the spectral reflectance difference between near infrared (NIR) band and red band. The NDVI values vary between − 1.0 and 1.0, where higher values indicate green vegetation.
- The NDVI of landsat8-9 was drawn against $C_{\text{Hydro.Arish}}$ and an equation between them was generated through regression analysis (Fig. 5c).

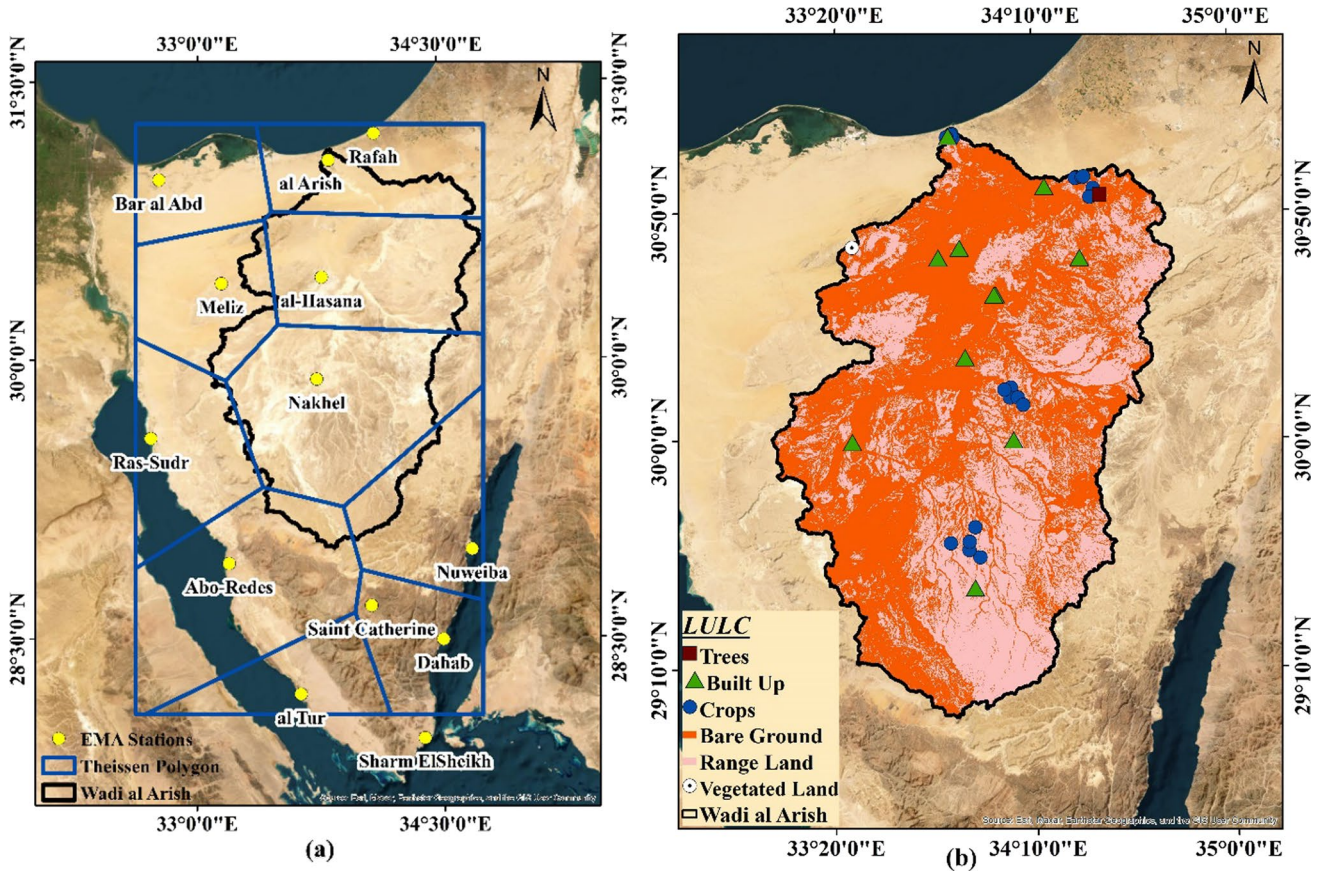

Fig. 4 Data collection of Wadi al-Arish, Sinai Peninsula, Egypt. **a** The Thiessen polygon for rainfall stations. **b** Sentinel-2 LULC, Jan, 2023

- The Derna basin in Libya was used to verify the proposed equation.
- C_{SA}; represents the cover management factor determined by relating the NDVI-Landsat 8–9 of Wadi Derna to the proposed equation.
- The C-Factor for semi-arid basins (C_{SA}) values were mapped to verify the accuracy of the proposed equation.
- The tropical cover management factor (C_{TR}) and the European cover management factor (C_{EU}) were calculated using Eqs. 1 of Colman et al. (2019) and Eqs. 2 of Der Knijff et al. (2000), respectively by applying the NDVI Landsat 8–9 satellite data of Wadi Derna.

$$C_{TR} = 0.1\left(\frac{-\mathrm{NDVI}+1}{2}\right) \tag{1}$$

$$C_{EU} = \exp\left(-\alpha\frac{\mathrm{NDVI}}{\beta-\mathrm{NDVI}}\right). \tag{2}$$

Here α and β are two parameters usually take the values of 2 and 1, respectively.

- $C_{\mathrm{Hydro.Derna}}$; represents the cover management factor simulated by the hydrological model within the verification basin of Wadi Derna, Libya.
- The values of C_{SA}, C_{TR}, and C_{EU} were calibrated with the hydrological values $C_{\mathrm{Hydro.Derna}}$ using statistical parameters. The correlation coefficient (r) is used to assess the agreement between the hydrological results and the calculated values, the r value close to + 1 indicates a perfect positive fit, while the relative bias in percent (RBIAS) measures the average tendency of the calculated values to be larger or smaller than their reference ones. The optimal value of RBIAS is 0.0. Its acceptable range is ± 25%. The Root Mean Square Error (RMSE) indicates the average difference between the hydrological outputs and the calculated data. Also, the Index of agreement (d) is used as a unit to measure the degree of error of the inferred values relative to the measured ones, which ranges from zero to one, where the degree of agreement increases as it approaches unity (Willmott 1981).

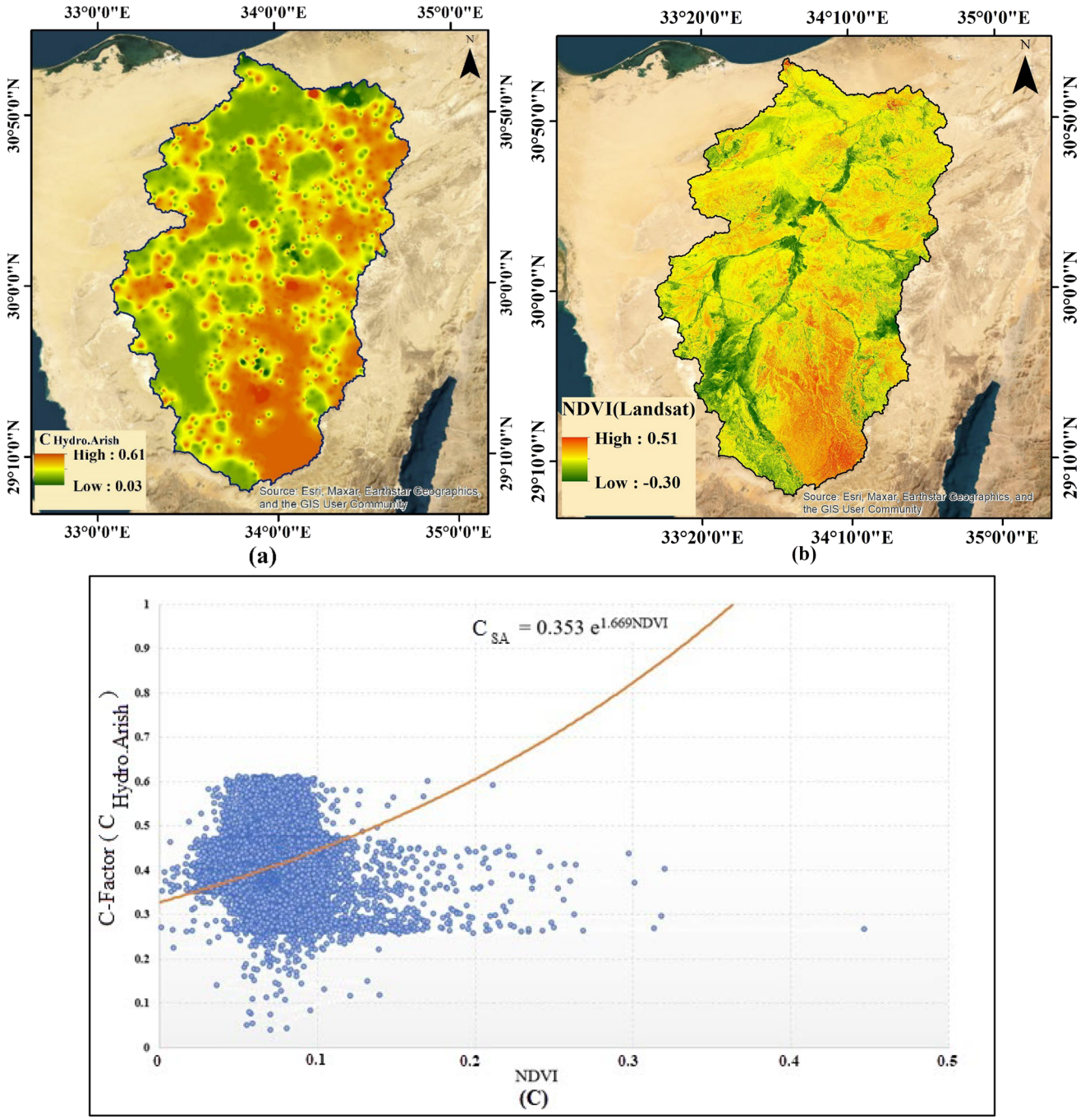

Fig. 5 **a** Simulation of $C_{\text{Hydro.Arish}}$, **b** NDVI of Landsat8-9, Jan, 2023, **c** relation between the C-factor and NDVI

$$r = \frac{n\sum\left(Z_o Z_s\right) - \left(\sum Z_o\right)\left(\sum Z_s\right)}{\sqrt{\left(n\sum\left(Z_s\right)^2 - \sum\left(Z_s\right)^2\right)\left(n\sum\left(Z_o\right)^2 - \sum\left(Z_o\right)^2\right)}} \quad (3)$$

$$\mathrm{RBIAS} = \frac{\sum_{i=1}^{n}\left(Z_s - Z_o\right)}{\sum_{i=1}^{n}\left(Z_o\right)} * 100 \quad (4)$$

$$\mathrm{RMSE} = \sqrt{\frac{\left(Z_o - Z_S\right)^2}{n}} \quad (5)$$

$$d = 1 - \frac{\sum_{i=1}^{n}\left(Z_o - Z_S\right)^2}{\sum_{i=1}^{n}\left(\left|\left|Z_S - Z_{o(avg)}\right|\right| + \left|\left|Z_o - Z_{o(avg)}\right|\right|\right)^2}. \quad (6)$$

In these equations, Z_o represents the values of $C_{\mathrm{Hydro.Derna}}$, $Z_{o(avg)}$ represents the mean value of $C_{\mathrm{Hydro.Derna}}$, and Z_s represents C_{SA}, C_{TR}, or C_{EU}.

Results and discussion

Hydrological analysis

The Soil Conservation Service–Curve Number (SCS-CN) method is applied to estimate the direct surface runoff from rainfall, it based on an empirical approach of the relationship between rainfall and ground conditions including soil types, moisture content, and land practices. The C-Factor was calculated using the CN, which depends on two basic factors: the vegetation type and the soil characteristics (Trinh et al. 2018). Vegetation type was defined as shown in Fig. 4b, while soil type was classified into group C which has a low infiltration rates. Table 1 shows that the values of CN decrease when the intensity of the land cover increases and vice versa, it reaches its lowest value in case of forests and dense trees, while its value increases in case of urban areas and barren lands with low intensity of land cover. The values of C-Factor is directly proportional to the values of CN, as the more surface runoff increases, the more soil erosion increases. Therefore, the values of the C-Factor increase in the case of barren lands and urban zones, where there is no vegetative protection, while it decreases in case of forests with high dense of land cover. The interaction between the type of vegetation and the soil characteristics affects the rate of soil loss as it helps to increase the ability to absorb water by creating pores that facilitate the entry of water deep into the soil. This helps provide groundwater and increase the percentage of green soil, also it increases the biodiversity, which helps to improve land fertility and increase agricultural productivity. So, vegetation cover and soil characteristics are considered the most important factors in preserving soil erodibility, and improving its fertility.

HEC-HMS hydrological software was used to compute the values of the C-Factor ($C_{\mathrm{Hydro.Arish}}$) for each land cover and curve number. These values vary between 0 and 1. It is observed that the greener the cover, the closer the coefficient to zero.

Large areas of semi-arid basins formed from barren lands due to the topographic nature, and steep slopes that distinguish semi-arid areas, resulting in the increase of flood events and the drift of large areas of agricultural lands. Also, most of NDVI values range from < 0.05 to 0.25 in barren lands and deserts (Ghebrezgabher et al. 2020). Therefore, NDVI, vegetation cover, and soil characteristics differ in semi-arid areas from those in tropical and European regions (Amara et al. 2022). An equation between the NDVI and the $C_{\mathrm{Hydro.Arish}}$ is shown in Fig. 5, to get the C-Factor for semi-arid basins (C_{SA}).

$$C_{SA} = 0.353e^{1.669\ \mathrm{NDVI}}, \quad e \text{ is the exponential function.} \quad (7)$$

Verification of the proposed equation

Derna Valley in Libya was chosen as one of the semi-arid valleys to ensure the validity of applying the C_{SA} Eq. (7) in semi-arid basins, the NDVI of the Landsat8-9 was applied

Table 1 Values of $C_{\mathrm{Hydro.Arish}}$ for land cover and curve number of Wadi al-Arish, Sinai, Egypt

Land cover	Curve number (CN)	$C_{\mathrm{Hydro.Arish}}$
Bare ground	85	0.47
Vegetated land	77	0.30
Dense trees/forest	55	0.03
Range land	80	0.35
Built in	90	0.61
Crops	75	0.26

Table 2 Values of $C_{\mathrm{Hydro.Derna}}$ for land cover and curve number of Wadi Derna, Libya

Land cover	Curve number (CN)	$C_{\mathrm{Hydro.Derna}}$
Bare ground	85	0.50
Vegetated land	80	0.35
Dense trees/forest	55	0.031
Range land	82	0.42
Built in	92	0.61
Crops	77	0.30

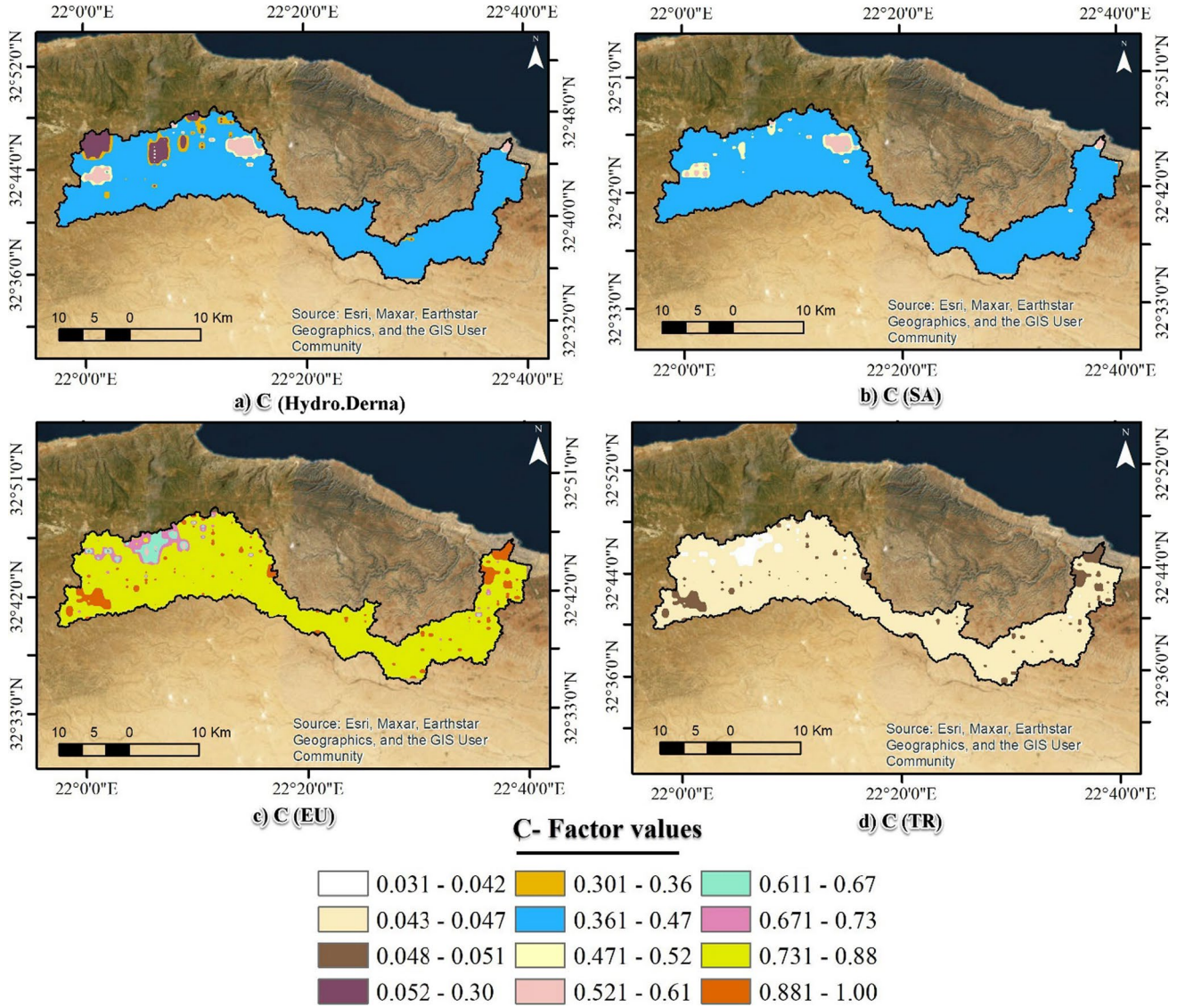

Fig. 6 Distribution of the four types of the C-Factor over Derna valley: **a** $C_{\text{Hydro.Derna}}$, **b** C_{SA}, **c** C_{EU}, **d** C_{TR}

to the C_{SA}, C_{TR}, and C_{EU} equations to get C-Factor values for the three different equations, then the values of the three C-Factors were calibrated with the cover management factor determined by the hydrological model ($C_{\text{Hydro.Derna}}$). Table 2 indicates that the hydrological results are close to the outputs of Wadi al-Arish in Sinai due to the similarity of the land covers and soil characteristics in semi-arid basins which are characterized by the dominance of bare soils and range lands.

Figure 6 shows the output of the Arc-GIS in which the values of the C-Factors are simulated over the basin area of Wadi Derna noting that the Inverse Distance Weighting (IDW) interpolation method was utilized to predict the unknown values for any geographic raster data. It is noticeable from the maps that the results of the C-Factor deduced from C_{SA} Eq. (7) are the closest to the C-Factor determined by the hydrological model ($C_{\text{Hydro.Derna}}$).

Table 3 Accuracy checks using statistical parameters

C-Factor	Statistical parameter			
	r	RBIAS%	RMSE	d
C_{SA}	0.702	0.50	0.049	0.768
C_{TR}	0.165	– 36.60	0.373	0.001
C_{EU}	0.163	39.80	0.409	0.02

Calibration and evaluation

Some of the well-known statistical parameters were used to check which of the three C-factors (C_{SA}, C_{TR}, C_{EU}) is the nearest to the $C_{Hydro.Derna}$ factor. Results in Table 3 show a directly correlation between the hydrological reference output ($C_{Hydro.Derna}$), and the cover management values calculated from C_{SA} equation than the other two C-Factors (C_{TR} and C_{EU}). The parameter (r) values equal to 0.702 for the $C_{SA,}$ and 0.2 for both the C_{TR} and the $C_{EU,}$ which indicates a better correlation between C_{SA} and $C_{Hydro.Derna}$ and means that the increase in C_{SA} is associated with the increase in $C_{Hydro.Derna.}$ Much better values of the RBIAS of C_{SA} of 0.50% (close to zero), and the RMSE has a small value of 0.049, which reflects the low error rate between the data, also the values of the statistical criteria (d) show a satisfactory agreement of C_{SA} than C_{EU} and the C_{TR}. Comparing these values with the values of r, d, RBIAS, and RMSE in cases of C_{TR} and C_{EU}, shows that C_{SA} equation is better be used to estimate the C-Factor in semi-arid basins.

By comparing the frequencies of 800 samples distributed within the catchment area between the hydrologically calculated C-Factor values ($C_{Hydro.Derna}$) and those calculated from the C_{SA}, C_{EU}, and the C_{TR} equations. Figure 7 shows that the frequencies of the C_{SA} values are the closest to the hydrological outputs, where the C_{SA} values are centered around 0.40 and 0.42, in which the values of C_{TR} and C_{EU} range from 0.03 to 0.05, and from 0.77 to 0.83, respectively. While, the mean value of $C_{Hydro.Derna}$ is 0.41. Also, Fig. 8 shows that the mean values of C_{SA}, C_{TR} and C_{EU} are 0.416, 0.045 and 0.809, respectively. This proves that C_{SA} equation estimates the value of C-Factor more accurately than Eqs. (1) and (2), the values below and above the ranges are the outliers.

Many trials were conducted varying the values of α and β in Eq. (2) to improve their results of C_{EU} compared with $C_{Hydro.Derna}$ values, but it was found that the best values of α and β are 2 and 1, respectively.

Findings of this study were compared to the aforementioned literatures, performed in semi-arid regions including; Tribak et al. (2009), Driss and Brahim (2018), Zakariae and Abdellatif (2021), and Okacha and Salhi (2023). The results showed a noticeable convergence between this study and literatures in most types of plant covers, such as crops, where literatures showed values ranged between 0.25 and 0.358. This study gave values equal to 0.26 and 0.30 for Wadi al-Arish and Derna, respectively. It also

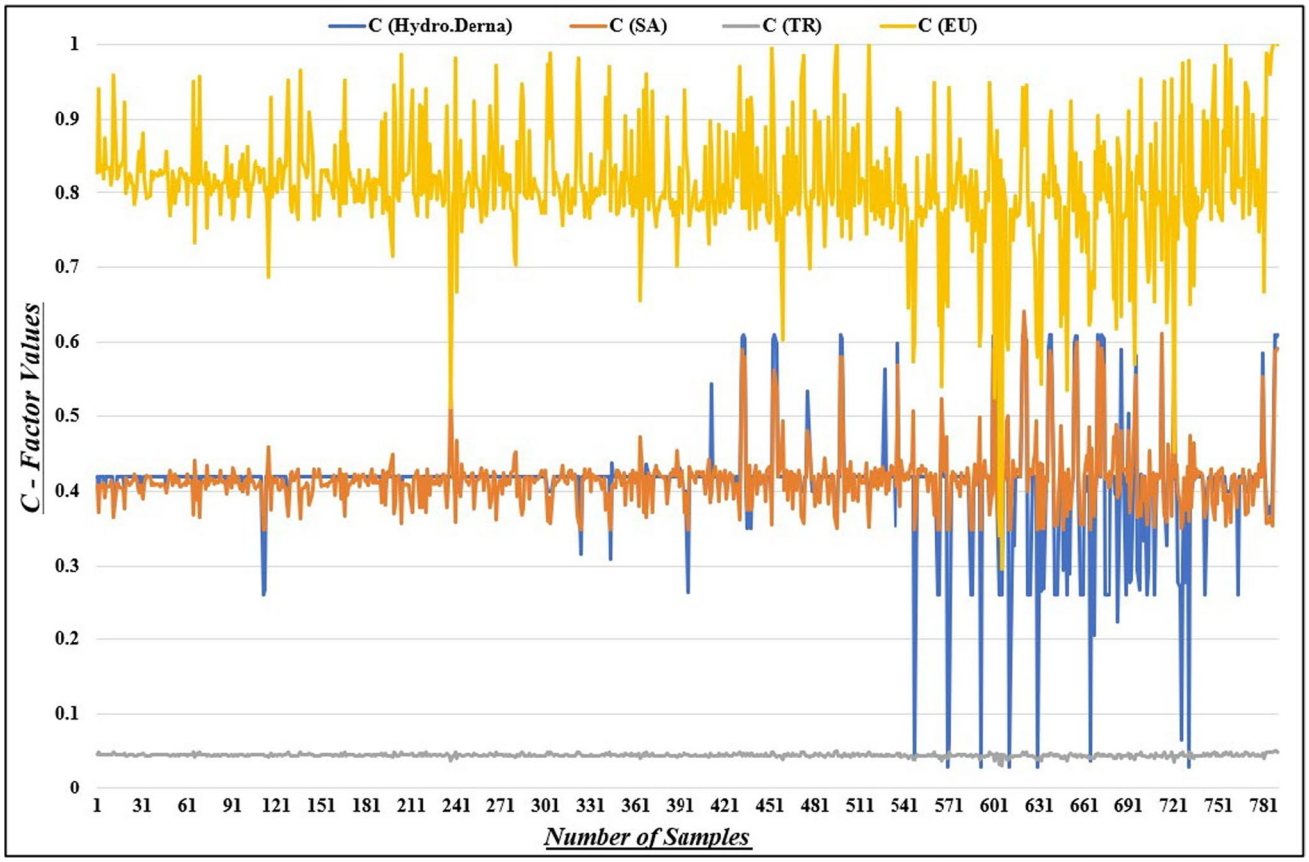

Fig. 7 Frequencies of $C_{Hydro.Derna}$ to C_{SA}, C_{TR} and C_{EU}

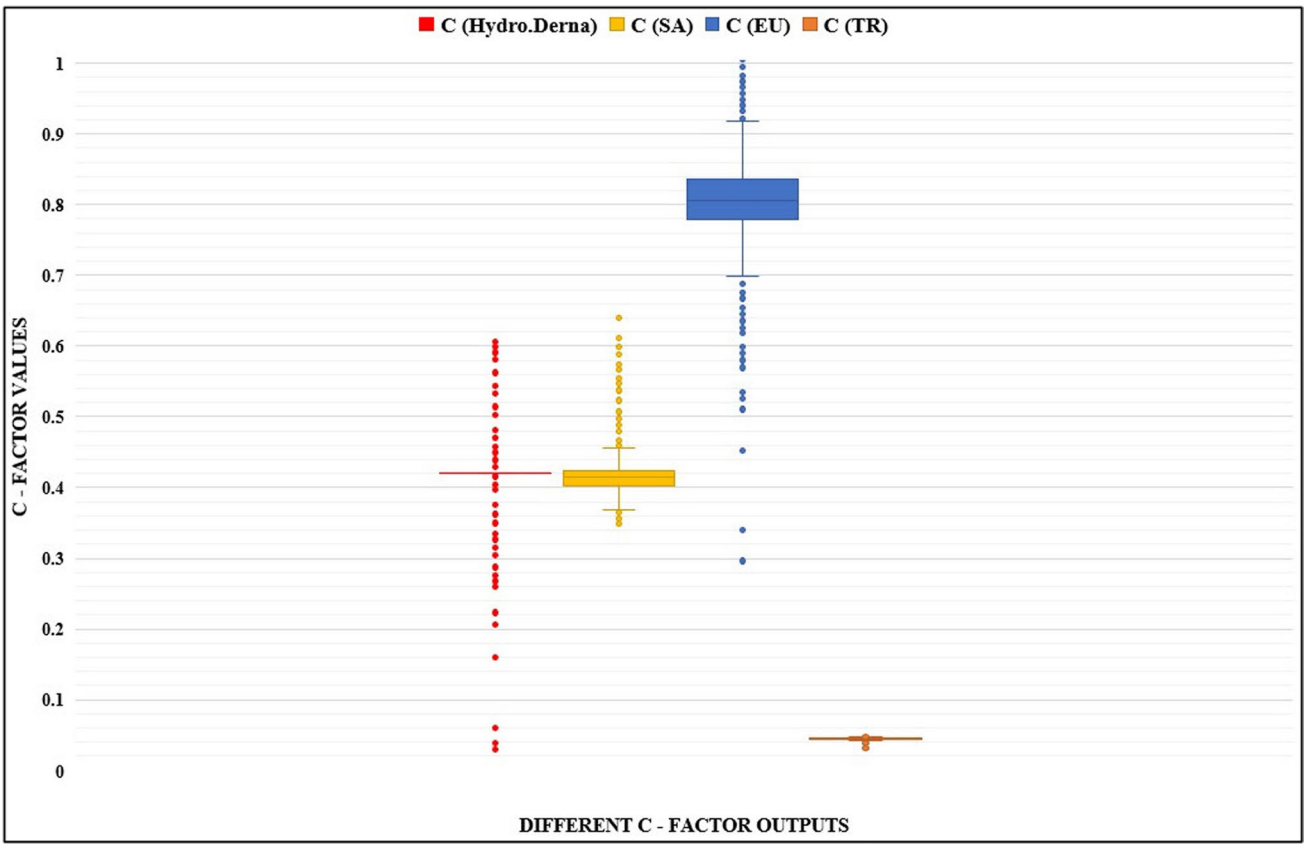

Fig. 8 Comparing $C_{\text{Hydro.Derna}}$ to C_{SA}, C_{TR} and C_{EU}

showed good results in vegetated lands, literatures showed results ranged from 0.26 to 0.59, while this study showed values of 0.30 and 0.35 for Wadi al-Arish and Wadi Derna, respectively. In forests, literatures ranged between 0.06 and 0.11, results gave values of 0.03 and 0.031 for Wadi al-Arish and Wadi Derna. However, results of the bare soil showed less agreement with Driss and Brahim (2018), Zakariae and Abdellatif (2021), and Okacha and Salhi (2023), but gave satisfactory results with Tribak et al. (2009), where literatures gave values of 0.55, 0.75, 0.75, and 0.70 for Tribak et al. (2009), Driss and Brahim (2018), Zakariae and Abdellatif (2021), and Okacha and Salhi (2023), respectively, while it appeared with values of 0.47 and 0.50 in Wadi al-Arish and Wadi Derna, respectively. It is noted that the values of the C-Factor for the bare soil are the highest in comparison with other land cover types, that is due to the lack of vegetative protection and the increase in surface runoff, which exposes them to a greater risk of soil erosion. In contrast, in case of forests, which had the lowest values among all vegetation cover types, due to dense land cover that increase resistance to runoff flow and the time of the water trip, giving more opportunity time for water to seep into the soil reducing runoff and decreasing the expected soil loss rates. See Table 4.

Table 4 Comparison of estimated C-Factor with literatures in semi-arid regions

Land cover type	Literatures C-Factor				Estimated C-Factor	
	Tribak et al. (2009)	Driss and Brahim (2018)	Zakariae and Abdellatif (2021)	Okacha and Salhi (2023)	Wadi al-Arish $C_{\text{Hydro.Arish}}$	Wadi Derna $C_{\text{Hydro.Derna}}$
Crops	0.28	0.25	0.25	0.358	0.26	0.30
Forests	0.08	0.08	0.11	0.06	0.03	0.031
Bare soil	0.55	0.75	0.75	0.70	0.47	0.50
Vegetated land	0.35	0.28	0.26	0.59	0.30	0.35

Summary and conclusions

Accurate estimation of soil erosion is one of the most essential tasks for researchers and civil engineers. The cover management factor (C-Factor) is a main parameter in the universal soil loss equation, it estimates the soil loss rates and the soil's ability to reduce the water's impulsive force. This factor is determined either using guiding tables or empirical equations derived from tropical and European conditions. However, these values are not suitable for semi-arid regions that have a different topography, nature, and climatic conditions. It is difficult to obtain the C-Factor as it needs long term monitoring soil erosion plots under natural rainfall. Therefore, this study combines the hydrological analysis as an alternative for obtaining the C-Factor in terms of NDVI derived from remote sensing approaches. The validity of the C-Factor depends on the accuracy of the NDVI values, which changes continuously in semi-arid areas due to the climate variability and extreme occurrences resulting from the lack of the vegetative protection. Therefore, morphological changes should be monitored by satellite images. However, it is always an important goal to get accurate satellite images with sufficient high resolution. Sentinel-2 satellite data of Wadi al-Arish in Sinai Peninsula in Egypt was used to simulate the land covers, and a regression equation was generated between the NDVI of landsat8-9 satellite product and the C-Factor inferred from hydrological modeling ($C_{\text{Hydro.Arish}}$) to get a semi-arid equation named C_{SA}. Moreover, the accuracy of the proposed equation was verified by applying the NDVI of landsat8-9 of Wadi Derna to the C_{SA}, C_{TR}, and C_{EU} equations developed in semi-arid, tropical, and European climates, respectively. Then, statistical analysis was used to calibrate the $C_{\text{Hydro.Derna}}$ values generated by the hydrological model at Wadi Derna against the C_{SA}, the C_{EU}, and the C_{TR}. The results showed that determining the C-Factor for semi-arid regions using the proposed C_{SA} equation is more accurate than determining it using tropical or European ones. Therefore, this study recommends using the derived semi-arid Eq. (7) to calculate the C-Factor in terms of the NDVI index in semi-arid catchments.

Author contributions All authors shared experiences, wrote and revised the manuscript in equal proportions.

Funding Open access funding provided by The Science, Technology & Innovation Funding Authority (STDF) in cooperation with The Egyptian Knowledge Bank (EKB). Open access funding is provided by the agreement between Springer Nature and Science, Technology & Innovation Funding Authority (STDF) in cooperation with Egyptian Knowledge Bank (EKB).

Data availability Not Applicable.

Declarations

Conflict of interest The authors declare no competing interests.

References

Amara DMK, Benya I, Kanu SA, Saidu DH, Musa RM, Vonu OS, Brima F, Mboma JCA, Jusu M, Turay F, Kamara A (2022) Effect of land uses on soil erodibility in the Njala Area of Southern Sierra Leone. Open J Soil Sci 12(10):475–489. https://doi.org/10.4236/ojss.2022.1210019

Ashoor A (2022) Estimation of the surface runoff depth of Wadi Derna Basin by integrating the geographic information systems and Soil Conservation Service (SCS-CN) model. Sebha Univ J Pure Appl Sci. https://doi.org/10.51984/JOPAS.V21I2.2137

Ayalew DA, Deumlich D, Šarapatka B, Doktor D (2020) Quantifying the sensitivity of NDVI-based C factor estimation and potential soil erosion prediction using spaceborne earth observation data. Remote Sens 12(7):1136. https://doi.org/10.3390/rs12071136

Balouei F, Mohammadi S, Kopaei SS (2021) Simulating the effects of land-use changes on soil erosion via RUSLE model in Ilam province's Doiraj Basin. Desert Ecosyst Eng J 10(31):59–70. https://www.magiran.com/paper/2334663/simulating-the-effects-of-land-use-changes-on-soil-erosion-via-rusle-model-in-ilam-province-s-doiraj-basin?lang=en

Centeri C (2022) Soil water erosion. Water 14(3):447. https://doi.org/10.3390/w14030447

Colman CB, Paulo TS, Oliveira AA, Britaldo SS-F, Dulce BBR (2019) Effects of climate and land-cover changes on soil erosion in Brazilian pantanal. Sustainability 11(24):7053. https://doi.org/10.3390/su11247053

Driss EH, Brahim A (2018) Quantification De L'erosion Hydrique En Utilisant Le Modèle Rusle Et Déposition Intégrée Dans Un Sig Cas Du Bassin Versant De L'oued Isly (Maroc Oriental). Eur Sci J ESJ 14(5):373. https://doi.org/10.19044/esj.2018.v14n5p373

El Afandi G, Morsy M, El Hussieny F (2013) Heavy rainfall simulation over Sinai Peninsula using the weather research and forecasting model. Int J Atmos Sci 2013:1–11. https://doi.org/10.1155/2013/241050

Ghebrezgabher MG, Yang T, Yang X, Eyassu Sereke T (2020) Assessment of NDVI variations in responses to climate change in the Horn of Africa. Egypt J Remote Sens Space Sci 23(3):249–261. https://doi.org/10.1016/j.ejrs.2020.08.003

Imamoglu A, Dengiz O (2017) Determination of soil erosion risk using RUSLE model and soil organic carbon loss in Alaca catchment (Central Black Sea region, Turkey). Rend Lincei 28(1):11–23. https://doi.org/10.1007/s12210-016-0556-0

Jiang Z, Huete AR, Chen J, Chen Y, Li J, Yan G, Zhang X (2006) Analysis of NDVI and scaled difference vegetation index

retrievals of vegetation fraction. Remote Sens Environ 101(3):366–378. https://doi.org/10.1016/j.rse.2006.01.003
Karaburun A (2010) Estimation of C factor for soil erosion modeling using NDVI in Buyukcekmece watershed. Ozean J Appl Sci 3(1):77–85
Kumawat A, Yadav D, Samadharmam K, Rashmi I (2021) Soil and water conservation measures for agricultural sustainability. Soil Moisture Importance. https://doi.org/10.5772/intechopen.92895
Lee G, Hwang J, Cho S (2021) A novel index to detect vegetation in urban areas using UAV-based multispectral images. Appl Sci 11(8):3472. https://doi.org/10.3390/app11083472
Majoro F, Wali UG, Munyaneza O, Naramabuye F-X, Nsengiyumva P, Mukamwambali C (2020) Soil erosion modelling for sustainable environmental management in Sebeya Catchment, Rwanda. J Water Resour Prot 12(12):1034–1052. https://doi.org/10.4236/jwarp.2020.1212062
Mu X, Qiu J, Cao B, Cai S, Niu K, Yang X (2022) Mapping soil erosion dynamics (1990–2020) in the Pearl River Basin. Remote Sens. https://doi.org/10.3390/rs14235949
Okacha A, Salhi A (2023) Novel climate-specic models for C-factor assessment: insights from the five-parameter logistic function, the De Martonne Index, and NDVI. Res Square. https://doi.org/10.21203/rs.3.rs-3672103/v1
Panagos P, Borrelli P, Meusburger K, Alewell C (2015) Estimating the soil erosion cover-management factor at the European scale. Land Use Policy 48(May):38–50. https://doi.org/10.1016/j.landusepol.2015.05.021
Sun J, Liu Y, Zhou T, Liu G, Wang J (2018) Soil conservation service on the Tibetan Plateau, 1984–2013. Earth Environ Sci Trans R Soc Edinb. https://doi.org/10.1017/S1755691018000609
Tribak A, El Garouani A, Abahrour M (2009) Évaluation quantitative de l'érosion hydrique sur les terrains marneux du PréRif oriental (Maroc): cas du sous-bassin de l'oued Tlata. Sécheresse 20(4):333–337. https://doi.org/10.1684/sec.2009.0205
Trinh T, Kavvas ML, Ishida K, Ercan A, Chen ZQ, Anderson ML, Ho C, Nguyen T (2018) Integrating global land-cover and soil datasets to update saturated hydraulic conductivity parameterization in hydrologic modeling. Sci Total Environ 631–632(February):279–288. https://doi.org/10.1016/j.scitotenv.2018.02.267
Van der Knijff JM, Jones RJA, Montanarella L (2000) Soil erosion risk assessment in Italy. European Communities, EUR 19022, 32:1–58. https://esdac.jrc.ec.europa.eu/ESDB_Archive/serae/GRIMM/italia/eritaly.pdf
Vasquez-Mendez R, Ventura-Ramos E, Oleschko K, Hernandez-Sandoval L, Angel M (2011) Soil erosion processes in semiarid areas: the importance of native vegetation. Soil Erosion Studies. https://doi.org/10.5772/23211
Willmott CJ (1981) On the validation of models. Phys Geogr 2:184–194. https://doi.org/10.1080/02723646.1981.10642213
Yu S, Du W, Zhang X, Hong Y, Liu Y, Hong M, Chen S (2023) Spatiotemporal changes in NDVI and its driving factors in the Kherlen River Basin. Chin Geogr Sci. https://doi.org/10.1007/s11769-023-1337-1
Zakariae A, Abdellatif T (2021) Cartographie de l'utilisation des sols et de l'érosion hydrique dans le bassin versant de l'Oued Lahdar (Prérif oriental-Maroc): Utilisation des données de la télédétection et du modèle RUSLE. Bollettino Della Assoc Ital Di Cartogr 171(4–20):4–20. https://doi.org/10.13137/2282-572X/33429
Almagro A, Caregnatto Thomé TC, Colman CB, Pereira RB, Marcato Junior J, Rodrigues DBB, Oliveira PTS (2019) Improving cover and management factor (C-factor) estimation using remote sensing approaches for tropical regions. Int Soil Water Conserv Res 7(4):325–334. https://doi.org/10.1016/j.iswcr.2019.08.005